

RSC Advances



This is an *Accepted Manuscript*, which has been through the Royal Society of Chemistry peer review process and has been accepted for publication.

Accepted Manuscripts are published online shortly after acceptance, before technical editing, formatting and proof reading. Using this free service, authors can make their results available to the community, in citable form, before we publish the edited article. This *Accepted Manuscript* will be replaced by the edited, formatted and paginated article as soon as this is available.

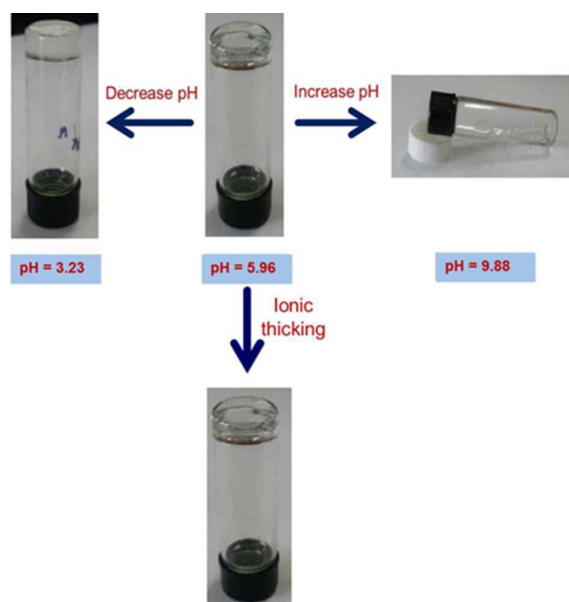
You can find more information about *Accepted Manuscripts* in the [Information for Authors](#).

Please note that technical editing may introduce minor changes to the text and/or graphics, which may alter content. The journal's standard [Terms & Conditions](#) and the [Ethical guidelines](#) still apply. In no event shall the Royal Society of Chemistry be held responsible for any errors or omissions in this *Accepted Manuscript* or any consequences arising from the use of any information it contains.

Abstract

Amphiphilic short peptides (ASPs) and surfactants (C14DMAO) were employed to prepare wormlike micelles. Herein, ASPs were used to induce wormlike micelles formation. The formation mechanism was investigated by cryo-TEM, FTIR, CD and rheometer. C14DMAO could be protonated by proton which was dissociated from the carboxyl headgroups of ASPs. The mean area of headgroup would reduced due to the interaction of protonated cationic surfactants and dissociated anionic ASPs which would lead to the wormlike micelles formation. And the length of wormlike micelles could be modulated by the size of hydrophobic part of ASPs. The wormlike micelles could also response to pH and metal ions, respectively. When pH was regulated from 5.96 to 3.23, the wormlike micelles transformed into nanofibers network. Nevertheless, when the pH was regulated over 9, spherical micelles would be formed and the solution would lose its viscoelasticity. When a certain amount of metal salts were added into the wormlike micelles solution with pH 5.96, the viscosity of solution increased significantly. The coordination interaction between metal ions and C14DMAO was considered as the responsive mechanism. Metal ions with high valence have more obvious effects on wormlike micelles.

Graphical abstract



**Amphiphilic short peptides modulated wormlike micelles
formation with pH and metal ions dual-responsive properties**

Dong Wang*^a, Yawei Sun^a, Meiwen Cao^a, Jiqian Wang*^a and Jingcheng Hao^b

*^aState Key Laboratory of Heavy Oil Processing & Centre for Bioengineering and
Biotechnology, China University of Petroleum (East China), Qingdao, 266580, China*

*^bKey Laboratory of Colloid and Interface Chemistry (Shandong University), Ministry
of Education, Jinan, 250100, China*

^a China University of Petroleum (East China)

^b Shandong University

CORRESPONDING AUTHOR E-mail: jqwang@upc.edu.cn

wangdong@upc.edu.cn

Abstract

Amphiphilic short peptides (ASPs) and surfactants (C₁₄DMAO) were employed to prepare wormlike micelles. Herein, ASPs were used to induce wormlike micelles formation. The formation mechanism was investigated by cryo-TEM, FTIR, CD and rheometer. C₁₄DMAO could be protonated by proton which was dissociated from the carboxyl headgroups of ASPs. The mean area of headgroup would reduced due to the interaction of protonated cationic surfactants and dissociated anionic ASPs which would lead to the wormlike micelles formation. And the length of wormlike micelles could be modulated by the size of hydrophobic part of ASPs. The wormlike micelles could also response to pH and metal ions, respectively. When pH was regulated from 5.96 to 3.23, the wormlike micelles transformed into nanofibers network. Nevertheless, when the pH was regulated over 9, spherical micelles would be formed and the solution would lose its viscoelasticity. When a certain amount of metal salts were added into the wormlike micelles solution with pH 5.96, the viscosity of solution increased significantly. The coordination interaction between metal ions and C₁₄DMAO was considered as the responsive mechanism. Metal ions with high valence have more obvious effects on wormlike micelles.

Key words: wormlike micelles, hydrogels, amphiphilic peptides, surfactants

Introduction

Wormlike micelles, long flexible aggregates of surfactant molecules in aqueous solution, are extremely simple yet highly versatile. Above a surfactant concentration threshold, the overlapping concentration (C^*), wormlike micelles entangle into a dynamic reversible network that is constantly breaking and reforming, for which they are also referred to as “living” or “equilibrium” polymers¹. The activation of the trigger enables the active, tailored tuning of the micellar structures and consequently of the associated rheological response². This emerging multidisciplinary field opens the door to a range of potential applications, including drag-reducing fluid^{3,4}, sensors⁵, microfluidics⁶, valves⁷, clean fracturing fluids⁸, tissue engineering⁹, heat transfer^{10,11}, personal care products¹², etc.

Wormlike micelles can be prepared by mixing salts^{13,14}, co-surfactant^{15,16} or another surfactant¹⁷⁻¹⁹ into surfactant solutions. The purpose of two components mixing is to increase the packing parameter $P = v/la$ by reducing the hydrophilic average area (a). Wormlike micelles would form at $1/3 < P < 1/2$. However, using ASPs as a participant to form wormlike micelles is reported seldom. ASPs are usually composed of hydrophobic amino acids as the hydrophobic tail and hydrophilic amino acids as the head. They can self-assemble into a variety of nanostructures²⁰⁻²³ including nanovesicles, nanotubes, nanobelts, nanoribbons, and nanofibers, etc., driven by the weak interactions such as electrostatic interaction, hydrogen bonds, hydrophobic interaction and van der Waals interaction. Because of the biocompatibility of peptides, nanomaterials of peptides could be well used in 3D cell or tissue culture, drug

delivery, food, cosmetics, environmental monitoring, etc^{24,25}. Therefore, it is significant to construct wormlike micelle systems that containing ASPs.

Abe et al. studied the formation and rheological behavior of viscoelastic wormlike micelles in mixed aqueous systems of acylglutamylsilacylglutamate (*m*-GLG-*m*, *m* = 12, 14 and 16) and cationic coamphiphile (C_nTAB, *n* = 14 and 16)²⁶. They thought the gemini amphiphile here forms wormlike micelles at lower molar volumes than its monomeric counterpart. They also used an amino acid-based surfactant (dodecanoylglutamic acid, C₁₂Glu) to form wormlike micelles by mixing with a tertiary alkylamine (dodecyldimethylamine, C₁₂DMA) or a secondary alkylamine (dodecylmethylamine, C₁₂MA)²⁷. Tirrell et al. design a peptide amphiphile (PA)²⁸. This PA could change its secondary structure of peptides headgroup which cause the wormlike micelle to spherical micelles transition.

Based on these previous works, in this article, we use conical ASPs as surfactant-like amphiphiles to induce the wormlike micelles formation in surfactant (tetradecyldimethylamine oxide, C₁₄DMAO) solution. We could modulate the wormlike formation by means of adjusting the volume of hydrophobic part of ASPs. Commercial surfactant, e. g. C₁₄DMAO, can synergistically act with amphiphilic peptides to form different structures. Hao et al. combined negative ASPs, A₆D, and C₁₄DMAO, to investigated the influence of surfactant on the self-assembly of amphiphilic peptides²⁹. Herein, we increased the concentration of C₁₄DMAO to investigate how the amphiphilic peptides induce the phase transition of C₁₄DMAO solutions. Meanwhile, the responsive properties of this complex system were also be

studied.

Experimental section

Materials

All the amphiphilic peptides were synthesized from ChinaPeptides Co. Ltd (purity>98%). C₁₄DMAO were provided by Prof. Jingcheng Hao as gifts (purity>98%). The deionized water used was from Millipore.

Sample preparation

40 mmol·L⁻¹ ASP was added into 200 mmol·L⁻¹ C₁₄DMAO to prepare wormlike micelles. HCl and NaOH was added by micropipettor and use pH meter to monitor pH value variation.

Circular Dichroism (CD)

The CD measurements were performed on a MOS-450 spectrometer (Biologic, France) using a 0.1 mm path-length quartz cuvette. The CD spectra were recorded at room temperature with wavelengths ranging from 190 to 300 nm and a scan speed of 50 nm·min⁻¹. The bandwidth was set to 0.5 nm, and an Xe lamp was used as the light resource. Using the Biokine software package, the solvent background was subtracted and the spectra could be smoothed. The resultant CD signals were expressed as [θ] (MilliDegree) versus wavelength

Scanning Electron Microscopy (SEM)

Gel samples were dried for 10 h under high vacuum after being frozen with liquid nitrogen. Then the samples were observed using a JEOL JMS-6700 SEM (Japan).

Transmission Electron Microscopy (TEM) and Cryogenic Transmission Electron

Microscopy (Cryo-TEM)

A drop of the sample ($\sim 4 \mu\text{L}$) at hydrogel state was placed on a TEM grid (copper grid, 3.02 mm, 200 meshes). Most of the liquid was removed with blotting paper leaving a thin film stretched over the holes. Then the copper grids were put in a vacuum extractor to remove water at $-50 \text{ }^\circ\text{C}$ for 24 h. The copper grids were observed through a JEOL JEM 1400 Plus TEM (Japan) at an accelerating voltage of 120 kV.

The cryo-TEM samples were prepared in a controlled environment vitrification system (CEVS). $\sim 4 \mu\text{L}$ sample solution was coated onto a TEM copper grid and the grid was blotted with two pieces of filter paper for about 4 seconds, leading to the formation of a solution thin film. Then, the grid was quickly plunged into a reservoir of liquid ethane ($-165 \text{ }^\circ\text{C}$, cooled by liquid nitrogen) and kept in liquid nitrogen until the observation. After transferring the grid to a cryogenic sample holder (Gatan 626) and putting the holder into a JEOL JEM-1400 Plus TEM (120KV) instrument at about $-174 \text{ }^\circ\text{C}$, one could observe the nanostructures.

Rheological Measurements.

Rheological measurements were performed on a Haake RS6000 rheometer with a coaxial cylinder sensor system. The viscoelastic properties were determined by oscillatory measurements from 0.01 to 100 Hz. In steady shear experiments, the shear rate was typically increased from 0.01 to 1000 s^{-1} in a step wise mode within approximately 10–35 min. To achieve equilibrium as far as possible, the rheometer was set to ensure the gradient was less than $0.5 (\Delta\tau/\tau)/\Delta t \%$ at each shear rate step, and the maximum waiting time was 60 s.

Small-Angle X-ray Scattering (SAXS)

Samples were prepared by placing a small amount of the hydrogel between two circular Teflon sheets (diameter 2 cm), compressing them, and then placing them in a sample holder. After SAXS analysis the samples were still in the hydrogel phase, with no visibly observable structural breakdown. The samples of dry gel were prepared in the same way. SAXS measurements were conducted at an HMBG-SAX system (Austria) with Ni-filtered Cu K α radiation (0.154 nm) operating at 50 kV and 40 mA.

Other instrumental characterization

Fourier Transform Infrared (FT-IR) spectra were obtained on a VERTEX-70/70v FT-IR spectrometer (Bruker Optics). Dynamic light scattering (DLS) measurements were carried out on a Malvern Zetasizer Nano ZS.

Results and discussion

The chemical structures of ASPs and the surfactants are shown in Figure 1. Hydrophobic part of LIVAGD, LIVAD, IVAD and IVD molecules are conical with the large cross section end far away from hydrophilic group, whereas hydrophobic part of AAAAAD molecule is cylindrical. The wormlike micelles were prepared by mixing these ASPs and surfactants in water with different concentrations at room temperature under weak acid environment. Pure 200 mmol·L⁻¹ C₁₄DMAO was spherical micelles in aqueous³⁰. When a certain amount (40 mmol L⁻¹ concentration was found to be optimal after a few attempts) of ASPs were added into 200 mmol·L⁻¹ C₁₄DMAO

solutions, the spherical micelles grew into long wormlike micelles. The growth of C_{14} DMAO micelles was induced by the interaction between C_{14} DMAO and ASPs. According to the critical packing parameter³¹, P_c ($P_c = v/l_c a_0$), where v is the volume of the hydrophobic tail, l_c is the maximum extended chain length and a_0 is the interfacial area occupied by the headgroup, the packing parameter was expected to increase towards $P_c = 1/3-1/2$, when the transition from spherical micelles to wormlike micelles. Therefore, either the increase of v or decrease of a_0 would lead to the increase of P_c .

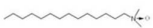
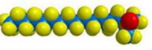

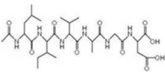
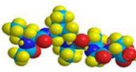
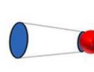
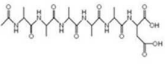
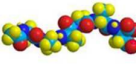
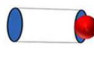
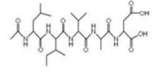
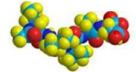
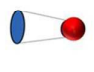
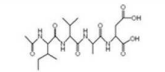
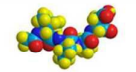
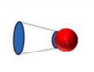
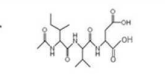
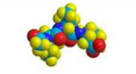
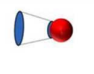
	Molecular Formula	Structural Formula	Abbreviation	Configuration
a			C_{14} DMAO	
b			LIVAGD	
c			AAAAAD	
d			LIVAD	
e			IVAD	
f			IVD	

Figure 1. Table for molecular formula, structural formula, molecular abbreviation and molecular configuration.

Firstly, the headgroup interaction of C_{14} DMAO and ASPs would decrease the parameter a_0 . C_{14} DMAO is known to be weak alkaline in aqueous solution, therefore when acid molecules are added in C_{14} DMAO solution, C_{14} DMAO would be

protonated and produce cationic surfactant $C_{14}DMAOH^+$ (Figure 2A). In order to examine this transition, Fourier transform infrared spectrum (FT-IR) was used³². The formation of cationic $C_{14}DMAOH^+$ with $C-N \rightarrow OH^+$ at low pH could increase the force constant of the bond, which is responsible for the band shift toward higher frequency upon protonation of the headgroup. Peaks between 1180 and 1250 cm^{-1} are attributed to the antisymmetric stretching of $C-N \rightarrow O$. as shown in Figure 2B, the intensity of absorption peaks near 1220 cm^{-1} increases when LIVAGD added, indicates the degree of protonation of $C_{14}DMAO$ becomes higher with the addition of acid molecule. After the protonation process, the nonionic surfactant translated into cationic surfactant and the peptides would be negative charged because of the losing of proton. The interaction of cation and anion between headgroups could lead to the reduction of mean area of headgroup (a_0).

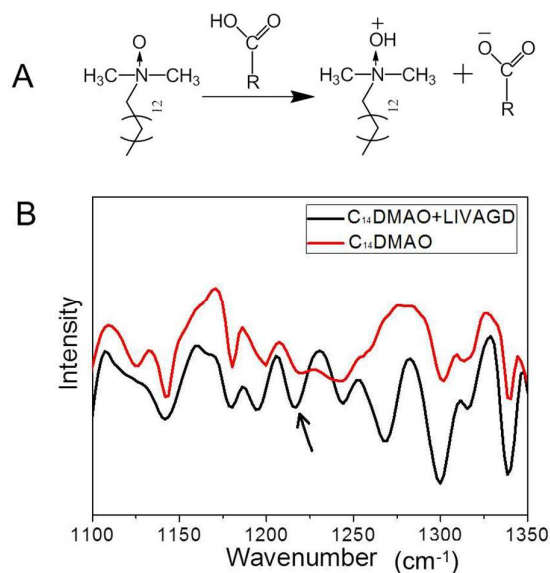


Figure 2. Protonation process of $C_{14}DMAO$ (A); FTIR spectrum for proving protonation of $C_{14}DMAO$ (B).

Secondly, the volume of hydrophobic part (v) also played important roles in the formation of wormlike micelles due to the ASPs have larger hydrophobic chain compared to alkane long chain of conventional surfactants. From cryo-TEM images in Figure 3 (A and B), molecules with larger hydrophobic tails, LIVAGD and AAAAAD could form long and dense wormlike micelles. However, with the size decreasing of hydrophobic part, LIVAD, IVAD and IVD (Figure 3C, D and E, respectively) molecule formed short and sparse wormlike micelles.

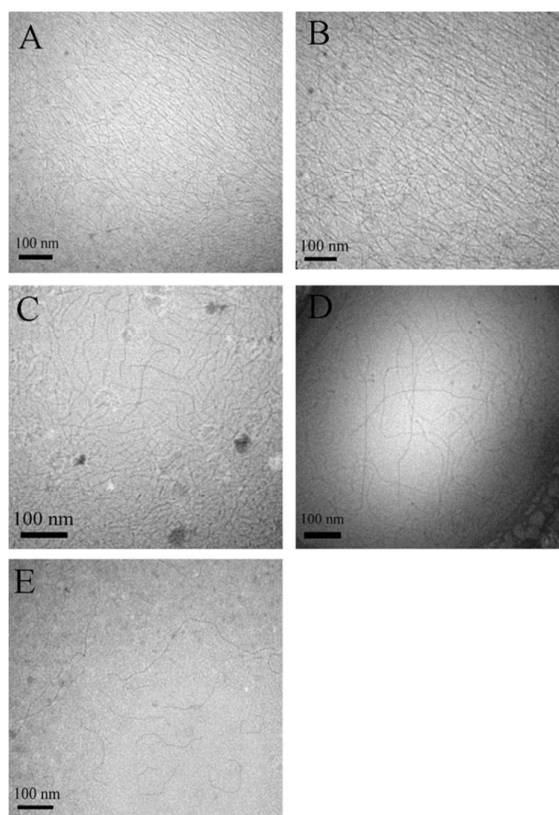


Figure 3. Cryo-TEM images of wormlike micelles formed by $200 \text{ mmol}\cdot\text{L}^{-1}$ C_{14}DMAO and $40 \text{ mmol}\cdot\text{L}^{-1}$ LIVAGD(A), AAAAAD(B), LIVAD(C), IVAD(D) and IVD(E).

CD spectrum (Figure 4A) shows that ASPs molecules are random coil condition in

surfactant solutions. That is because, the two carboxylic acids are negative charged when pH changed to about 6 (Aspartic Acid $pK_{\alpha} = 2.09$ and $pK_{\beta} = 3.86$, respectively). More C_{14} DMAO with positivity charge would be attracted around the negative carboxylic acids as shown in Figure 4B. Thus, the existence of C_{14} DMAO hinders the intermolecular hydrogen bonding formation of ASPs. Therefore, it could be assumed that ASPs molecules were inserted into surfactant aggregates with the headgroups exposed to the aqueous phase and hydrophobic part solubilized in hydrophobic core (Figure 4B).

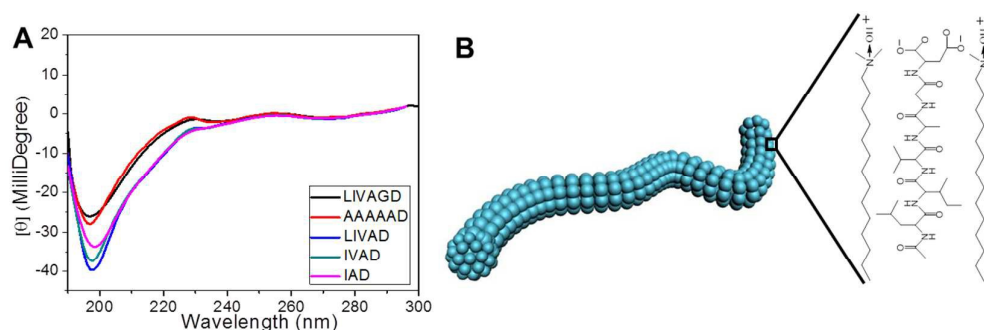


Figure 4. CD spectrum of $200 \text{ mmol}\cdot\text{L}^{-1}$ C_{14} DMAO and different ASPs (A); schematic cartoon of wormlike micelles formation (B).

The rheological properties of wormlike micelle solutions have been investigated by rheometer. The results were in accordance with Maxwell's mechanical model at low shear frequency which was reported by Cates *et al.*³³, a model to be used to describe living polymers (e.g. wormlike micelles). The storage modulus G' and the loss modulus G'' obey the following equations, which considered a single stress relaxation time τ_R :

$$G'(\omega) = G_0 \frac{\omega^2 \tau_R^2}{1 + \omega^2 \tau_R^2} \quad (1)$$

$$G''(\omega) = G_0 \frac{\omega \tau_R}{1 + \omega^2 \tau_R^2} \quad (2)$$

Where ω , represents angular frequency (here we use frequency, f , as an independent variable, that $\omega = 2\pi f$). G_0 and τ_R are high frequency plateau modulus and relaxation time, respectively. G_0 and τ_R can be obtained from the critical angular frequency (ω^*) and modulus (G^*) at which the curve of G' and G'' intersects according to the equations:

$$\tau_R = 1/\omega^* \quad (3)$$

$$G_0 = 2G^* \quad (4)$$

As shown in the set of diagrams in Figure 5 A to E, the decrease of hydrophobic part of ASPs leads to the increase of ω^* value (crossover point of G' and G''), indicates the shortened stress relaxation time (τ_R , see Table 1). It shows that the entangling of wormlike micelles was more relaxed with the decreasing of hydrophobic part of ASPs.

The viscosity (η) has a plateau value (so-called zero-shear viscosity, η_0), which represents the process of disentanglement (Figure 5F). And the zero-shear viscosity value (η_0) is lower (see Table 1) with the decreasing of hydrophobic part of ASPs. It was coincided with the cryo-TEM images (Figure 3), where a lot of short wormlike micelles were observed, when the hydrophobic part of ASPs were decreasing.

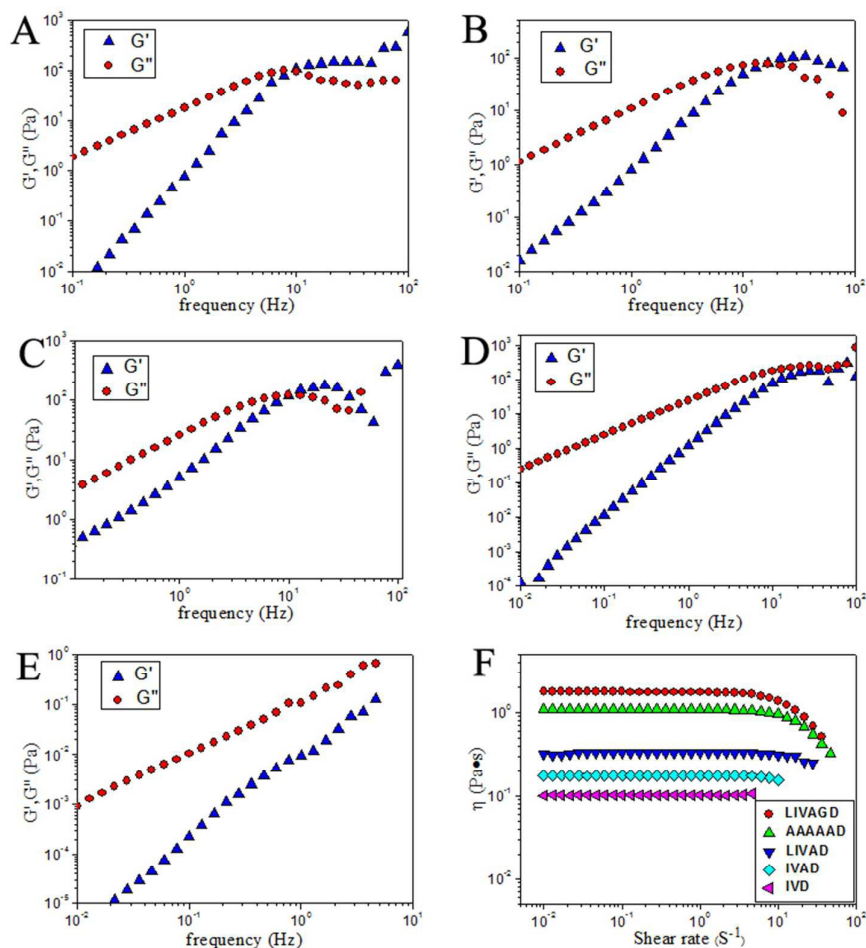


Figure 5. Rheology properties of $200 \text{ mmol}\cdot\text{L}^{-1}$ C_{14}DMAO and $40 \text{ mmol}\cdot\text{L}^{-1}$ LIVAGD (A), AAAAAD(B), LIVAD(C), IVAD(D) and IVD(E); steady shear experiments of $200 \text{ mmol}\cdot\text{L}^{-1}$ C_{14}DMAO and $40 \text{ mmol}\cdot\text{L}^{-1}$ ASPs (F).

The properties of wormlike micelles are determined by their structures, especially the average contour length of wormlike micelles, which is generally represented by the Maxwell fluid behavior:

$$\frac{G''_{min}}{G'_{\infty}} \approx \frac{l_e}{L_c} \quad (5)$$

where L_c is the average contour length and l_e is the average length between two entanglement points. G''_{min} is the minimum of loss modulus in the high frequency

region and G'_{∞} is the plateau modulus of storage modulus. Although, l_e is not currently available, as a comparison, a typical value of 80–150 nm for wormlike micelles can be adopted^{34,35} to estimate L_c . The L_c statistics from cryo-TEM and calculated from rheometer are both listed in Table 1. The L_c data indicates that the average contour length are decreased with the decrease of hydrophobic part of ASPs. L_c (rheometer) of AAAAAD is bigger than that of LIVAGD, which indicates that AAAAAD is more beneficial to wormlike micelles formation than the corresponding conical peptide LIVAGD.

Table 1. Rheology parameters of 200 mmol·L⁻¹ C₁₄DMAO and 40 mmol·L⁻¹ ASPs.

	LIVAGD	AAAAAD	LIVAD	IVAD	IVD
τ_R/s	0.13	0.09	0.1	0.02	—
$\eta_0/ Pa\cdot s$	1.9	1.0	0.35	0.2	0.1
L_c/ nm (Cryo-TEM)	>1000	>1000	700-900	400-600	200-400
G''_{min}/G'_w	0.2	0.12	0.45	~1	—
L_c/ nm (Rheometer)	400-750	667-1250	178-333	80-150	—

Several stimulus-responsive properties has been showed by the system of 200 mmol·L⁻¹ C₁₄DMAO and 40 mmol·L⁻¹ ASPs, such as pH-thickening, pH-thinning and metal ionic thickening (Figure 6).

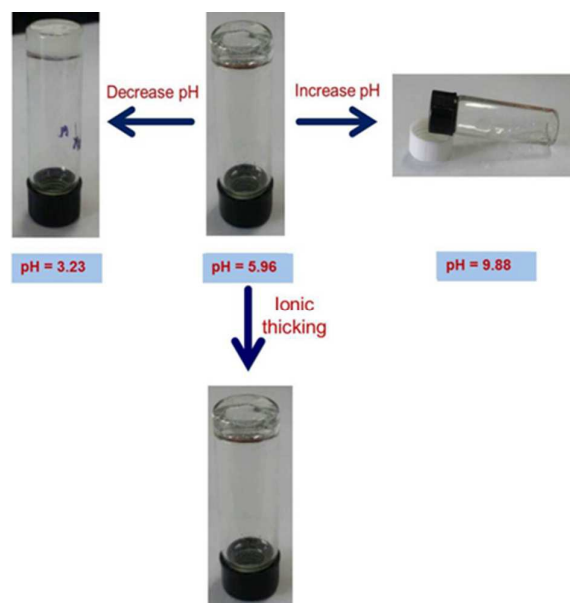


Figure 6. Schematic illustration of multiple-stimulus responsive wormlike micelles.

Because of the two carboxyl groups on aspartic residue, we found that the ASPs and C_{14} DMAO wormlike micelle systems could respond to pH variation. However, ASPs with larger hydrophobic part changed significantly. Therefore, LIVAGD was chosen as an example to explain the mechanism of transition. When pH was above 9.88, viscoelastic wormlike micelles changed into spherical micelles and the solution lose its viscoelastic properties. It can be assumed that, when pH increased, the charge situation of C_{14} DMAO will be changed. C_{14} DMAO is a nonionic surfactant in aqueous alkaline medium. The headgroup interaction between C_{14} DMAO and ASPs is not strong as that of in aqueous acidic medium. Therefore, spherical micelles are the main aggregates in this condition (see in Figure 7 A and B). DLS showed the diameter of spherical micelles was about 3-4 nm (Figure 7A), and it was in accordance with the cryo-TEM result in Figure 7B.

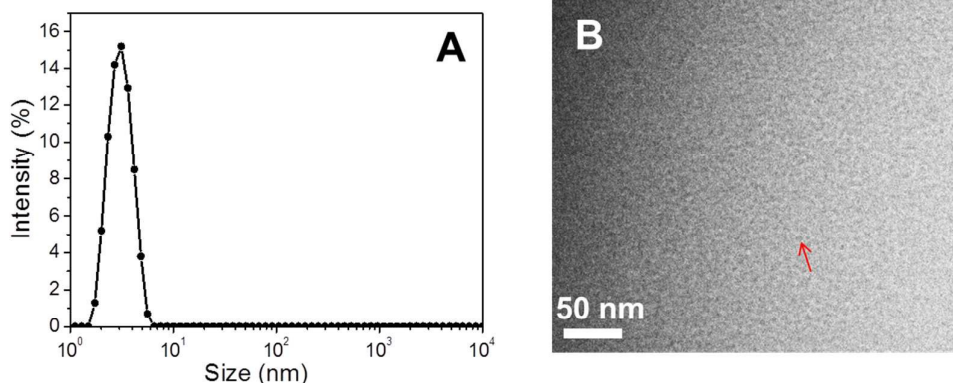


Figure 7. DLS (A) and Cryo-TEM images (B) of 200 mmol·L⁻¹ C₁₄DMAO and 40 mmol·L⁻¹ LIVAGD at pH = 9.88.

When pH below 3.23, the transparent hydrogels changed into turbid hydrogels (Figure 6). The microstructure of turbid hydrogels has been characterized by TEM, SEM, SAXS and CD. According to the TEM and SEM images (Figure 8 A and B), the turbid hydrogels are consist of nanobelts with the width of about 200 nm. SAXS (Figure 8C) curve has two peaks with the ratio about 1:2 which indicate that nanobelts composed of lamellar structures. The *d*-spacing (distance of lamellar structures), which can be calculated by Bragg equation, is about 4.18 nm. The molecule length (*l*) of C₁₄DMAO can be estimated as 2.05 nm from the equation $l = 1.5 + 1.265N$. And the length of LIVAGD obtained from previous references^{21,36} was about 1.8 nm. The data from SAXS (4.18 nm) was basically accordance with the estimated addition data of C₁₄DMAO and LIVAGD (2.05nm + 1.8nm = 3.85nm). CD spectrum indicated β -sheet formed at pH = 3.23. Hauser *et al.* explained the formation of hydrogel was caused by the anti-parallel arrangement of LIVAGD^{36,37}. Therefore, according to SAXS and CD measurements, we considered the ASPs and C₁₄DMAOH⁺ molecules

arranged as shown in Figure 8E. ASPs molecules arranged by adopting anti-parallel forms and $C_{14}DMAOH^+$ molecules around the ASP molecules depend on electrostatic interaction. Due to the decrease of pH to 3.23, ASPs carried less charge than that at pH = 5.96. Only α -carboxyl group was still charged ($pK_{\alpha} = 2.09$), with β -carboxyl group remains no change ($pK_{\beta} = 3.86$). Therefore, the interaction between ASPs and $C_{14}DMAOH^+$ molecules was weakened. And the interaction between ASPs and ASPs molecules was enhanced due to the absence of $C_{14}DMAOH^+$ disturbance around ASPs.

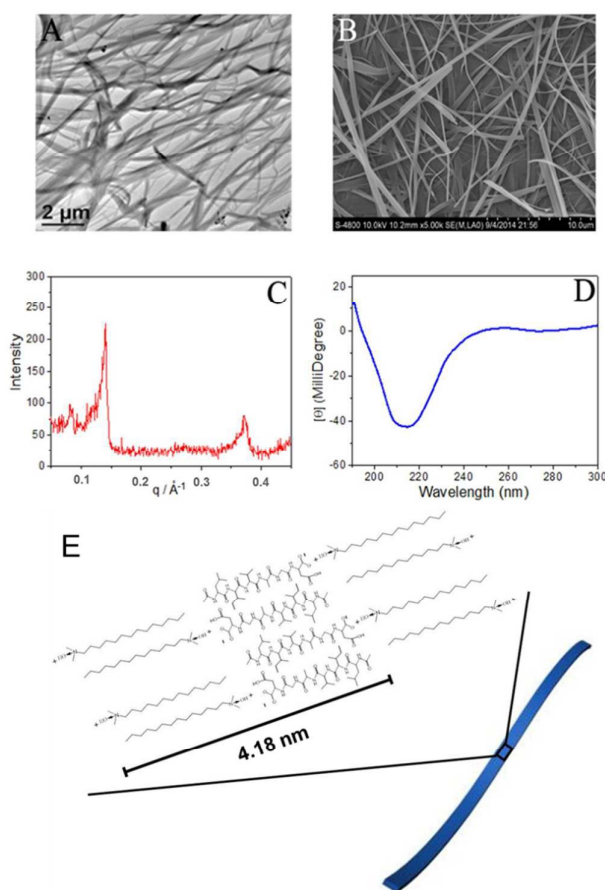


Figure 8. TEM(A), SEM (B) SAXS (C) and CD (D) measurements of $200 \text{ mmol}\cdot\text{L}^{-1}$ $C_{14}DMAO$ and $40 \text{ mmol}\cdot\text{L}^{-1}$ LIVAGD at pH = 3.23; schematic cartoon of nanobelts formation (E).

The rheological properties of turbid hydrogels were investigated by rotary rheometer. The results showed that the viscoelastic property of turbid hydrogels was different from that of transparent hydrogels. G' is 10 times larger than G'' without crosspoint in our measurement range. G' is about 70 Pa and G'' is about 7 Pa. The complex viscosity (η^*) decreased linearly over the whole measurement range. Steady shear viscosity (η) also decreased linearly with the increasing of shear rate. These rheological behaviors clearly indicated the viscoelastic properties of turbid hydrogels were solid-like hydrogel systems (or “strong” hydrogels), comparing to wormlike micelle systems which were also called liquid-like hydrogel system (or “weak” hydrogels).^{38,39}

According to pH responsive properties, a pH switchable fluid-solid transition was designed. The viscosity of fluid could be continuously adjusted by HCl and NaOH. When the pH decrease to 3 around, the viscosity reached to above 10^3 Pa·s, whereas when the pH return to 6 around, the viscosity decreased to about 2 Pa·s. Further adjust the pH to 9 around led the viscosity to be lowered to 0.1 Pa·s. This variation of viscosity was stable and repetitive even after 12 times of pH adjustments. (Figure 9C)

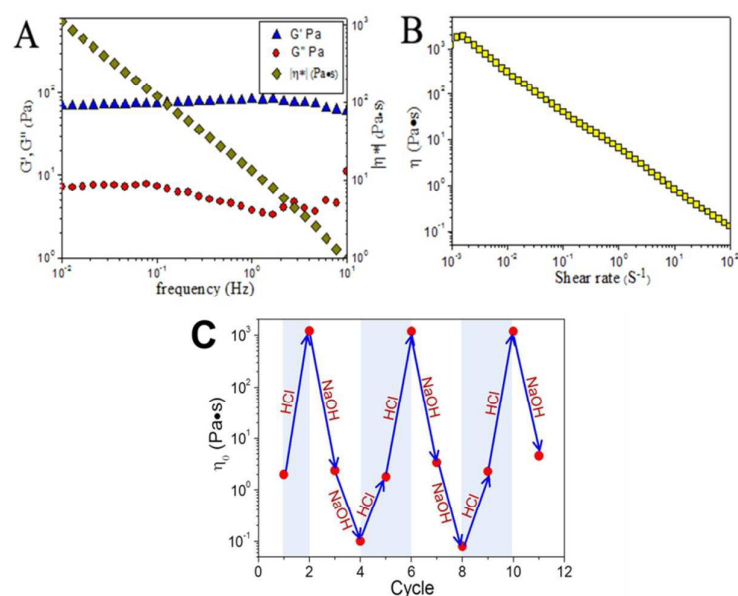


Figure 9. Viscoelastic property (A) and steady shear experiment (B) for $200 \text{ mmol}\cdot\text{L}^{-1}$ C_{14}DMAO and $40 \text{ mmol}\cdot\text{L}^{-1}$ LIVAGD at $\text{pH}=3.23$; pH cycle scheme of $200 \text{ mmol}\cdot\text{L}^{-1}$ C_{14}DMAO and $40 \text{ mmol}\cdot\text{L}^{-1}$ LIVAGD (C).

C_{14}DMAO and metal ions have strong coordinating interaction according to previous work^{40,41}. Therefore, metal ions would have effect on properties of wormlike micelles of C_{14}DMAO and ASPs. In order to examine this behavior, a set of experiments was designed: firstly, NaCl was added into wormlike micelle solutions of C_{14}DMAO and LIVAGD. It was found that the viscosity increased with increase of concentration of NaCl. The addition of NaCl raised viscosity more than 3 times (Figure 10A). Secondly, Other metal ions were also investigated. We found metal ions with higher valence had better effect on increasing viscosity of wormlike micelles., The addition of divalent metal ions and trivalent metal ions further increased the viscosity of wormlike micelles 10 and 25 times, respectively. However, the detailed

mechanism of metal ions effect is still not clear. System researches on metal ion effects will be presented in our future work.

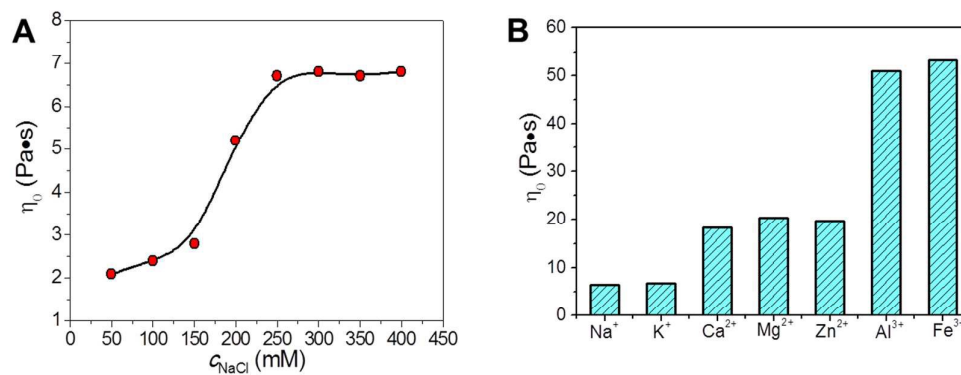


Figure 10. Zero-shear viscosity as a function of concentration of NaCl (A); viscosity increasing effect by different metal ions (B).

Conclusions

The combination of ASPs and C₁₄DMAO complexes formed wormlike micelles in aqueous solution. The structure of ASPs had significant effect on the properties of wormlike micelles. ASPs with larger hydrophobic part was beneficial to the formation of wormlike micelles. These wormlike micelles transformed into nanobelts networks when pH was decreased and spherical micelles when pH was increased. The transitions were regulated by charge variation of ASPs and C₁₄DMAO which was induced by pH changing. These wormlike micelles also have ionic thickening property.

Acknowledgements

This work was supported by China Postdoctoral Science Foundation (Project No. 2014M561979), Fundamental Research Funds for the Central Universities (Project No.14CX02126A and 14CX05040A), and National Natural Science Foundation of

China (Project No. 21473255)

References

- 1 S. Ezrahi, E. Tuval and a Aserin, *Adv. Colloid Interface Sci.*, 2006, **128-130**, 77–102.
- 2 L. M. Walker, *Curr. Opin. Colloid Interface Sci.*, 2001, **6**, 451–456.
- 3 K. Gasljevic and E. F. Matthys, *Energy Build.*, 1993, **20**, 45–56.
- 4 K. Gasljevic, G. Aguilar and E. F. Matthys, *J. Nonnewton. Fluid Mech.*, 2001, **96**, 405–425.
- 5 K. Tsuchiya, Y. Orihara, Y. Kondo, N. Yoshino, T. Ohkubo, H. Sakai and M. Abe, *J. Am. Chem. Soc.*, 2004, **126**, 12282–12283.
- 6 Y. Zhao, P. Cheung and A. Q. Shen, *Adv. Colloid Interface Sci.*, 2014, **211**, 34–46.
- 7 A. M. Ketner, R. Kumar, T. S. Davies, P. W. Elder and S. R. Raghavan, *J. Am. Chem. Soc.*, 2007, **129**, 1553–1559.
- 8 B. Chase, W. Chmilowski, R. Marcinew, C. Mitchell, Y. Dang, K. Krauss, E. Nelson, T. Lantz, C. Parham and J. Plummer, *Oilf. Rev.*, 1997, **9**, 20–33.
- 9 Z. Chu and Y. Feng, *Chem. Commun.*, 2011, **47**, 7191–7193.
- 10 S. Ezrahi, E. Tuval and a. Aserin, *Adv. Colloid Interface Sci.*, 2006, **128-130**, 77–102.
- 11 H. Shi, W. Ge, H. Oh, S. M. Pattison, J. T. Huggins, Y. Talmon, D. J. Hart, S. R. Raghavan and J. L. Zakin, *Langmuir*, 2013, **29**, 102–109.
- 12 J. Yang, *Curr. Opin. Colloid Interface Sci.*, 2002, **7**, 276–281.
- 13 T. Imae and S. Ikeda, *J. Phys. Chem.*, 1986, **90**, 5216–5223.
- 14 P. A. Hassan, S. R. Raghavan and E. W. Kaler, *Langmuir*, 2002, **18**, 2543–2548.
- 15 S. Kumar, H. N. Singh and P. S. Goyal, *Langmuir*, 1994, **10**, 4069–4072.

- 16 S. Kumar and P. S. Goyal, *Langmuir*, 1996, **12**, 1490–1494.
- 17 H. Hoffmann, A. Rauscher, M. Gradzielski and S. F. Schulzt, 1992, 2140–2146.
- 18 L. Ziserman, L. Abezgauz, O. Ramon, S. R. Raghavan and D. Danino, *Langmuir*, 2009, **25**, 10483–10489.
- 19 D. P. Acharya and H. Kunieda, *Adv. Colloid Interface Sci.*, 2006, **123-126**, 401–413.
- 20 Y. Yanlian, K. Ulung, W. Xiumei, A. Horii, H. Yokoi and Z. Shuguang, *Nano Today*, 2009, **4**, 193–210.
- 21 S. Zhang, *Acc. Chem. Res.*, 2012, **45**, 2142–2150.
- 22 X. Xu, J. Chen, H. Cheng, X. Zhang and R. Zhuo, *Polym. Chem.*, 2012, **3**, 2479-2486.
- 23 X. Xu, C. Chen, B. Lu, S. Cheng, X. Zhang and R. Zhuo, *J. Phys. Chem. B*, 2010, **114**, 2365-2372.
- 24 S. S. Santoso, S. Vauthey and S. Zhang, *Curr. Opin. Colloid Interface Sci.*, 2002, **7**, 262–266.
- 25 Z. Luo and S. Zhang, *Chem. Soc. Rev.*, 2012, **41**, 4736–4754.
- 26 R. G. Shrestha, K. Nomura, M. Yamamoto, Y. Yamawaki, Y. Tamura, K. Sakai, K. Sakamoto, H. Sakai and M. Abe, *Langmuir*, 2012, **28**, 15472–15481.
- 27 K. Sakai, K. Nomura, R. G. Shrestha, T. Endo, K. Sakamoto, H. Sakai and M. Abe, *Langmuir*, 2012, **28**, 17617–17622.
- 28 T. Shimada, S. Lee, F. S. Bates, A. Hotta and M. Tirrell, *J. Phys. Chem. B*, 2009, **113**, 13711–13714.
- 29 Y. Dou, H. Xu and J. Hao, *Soft Matter*, 2013, **9**, 5572-5579.
- 30 D. Wang, R. Dong, P. Long and J. Hao, *Soft Matter*, 2011, **7**, 10713-10719.
- 31 J. N. Israelachvili, D. J. Mitchell and B. W. Ninham, *Biochim. Biophys. Acta (BBA)-Biomembranes*, 1977, **470**, 185–201.
- 32 D. Wang, P. Long, R. Dong and J. Hao, *Langmuir*, 2012, **28**, 14155–14163.
- 33 M. E. Cates and S. M. Fielding, *Advances in Physics*, 2006, **55**, 799-879.

- 34 C. Rodriguez, D. P. Acharya, K. Hattori, T. Sakai and H. Kunieda, *Langmuir*, 2003, **19**, 8692–8696.
- 35 Y. Bi, H. Wei, Q. Hu, W. Xu, Y. Gong and L. Yu, *Langmuir*, 2015, **31**, 3789-3798.
- 36 A. Mishra, Y. Loo, R. Deng, Y. J. Chuah, H. T. Hee, J. Y. Ying and C. a E. Hauser, *Nano Today*, 2011, **6**, 232–239.
- 37 C. A. E. Hauser, R. Deng, A. Mishra, Y. Loo, U. Khoe and F. Zhuang, D. W. Cheong , A. Accardo , M. B. Sullivan, C. Riekel, J. Y. Ying, and U. A. Hauser *PNAS*, 2011, **108**, 1361-1366.
- 38 P. Terech and R. G. Weiss, *Chem. Rev.*, 1997, **97**, 3133–3160.
- 39 S. R. Raghavan, *Langmuir*, 2009, **25**, 8382–8385.
- 40 H. Tian, Q. Ding, J. Zhang, A. Song and J. Hao, *Langmuir*, 2010, **26**, 18652–18658.
- 41 H. Tian, D. Wang, W. Xu, A. Song and J. Hao, *Langmuir*, 2013, **29**, 3538–3545.